PNAS
www.pnas.org

Supporting Information (SI) for

Evidence for massive and recurrent toxic blooms of *Alexandrium catenella* in the Alaskan Arctic

Donald M. Anderson, Evangeline Fachon, Robert S. Pickart, Peigen Lin, Alexis D. Fischer, Mindy L. Richlen, Victoria Uva, Michael Brosnahan, Leah McRaven, Frank Bahr, Kathi Lefebvre, Jackie Grebmeier, Seth Danielson, Yihua Lyu, Yuri Fukai

Corresponding author: Donald M. Anderson
danderson@whoi.edu

This PDF file includes:

Supplemental Text

Water mass definitions

Seasonally, the circulation of the Chukchi shelf advects a variety of Pacific-origin water masses northward. During the cold months of the year, much of the shelf is characterized by very cold Newly-Ventilated Winter Water (NVWW), which is high in nutrient content. In the spring the water begins to warm by solar heating and/or mixing with newly arriving summer waters, and is known as Remnant Winter Water (RWW). There are two varieties of Pacific-origin summer water. Bering Summer Water (BSW) is comprised of Anadyr water and central Bering shelf water that mix in the vicinity of Bering Strait (1). This water mass is also relatively high in nutrients due to the Anadyr contribution. BSW is predominantly advected by the Central Channel Branch (2). The second summer water is the Alaskan Coastal Water (ACW) advected by the Alaskan Coastal Current (ACC). This is the warmest Pacific-origin water found in the Chukchi Sea, which is strongly stratified and generally nutrient poor. An additional water mass relevant to the study is the very fresh, near-surface water comprised of sea-ice melt, run off from the continent, and/or river water. While these components can be distinguished using chemical tracers, we do not have the ability to do so with our data, hence they are collectively considered as a single water type called meltwater / river runoff (MWR).

Toxin composition profiles

A useful approach to the study of the connectivity of geographically separated *Alexandrium catenella* populations is the analysis to toxin composition profiles for individual isolates from different regions. Saxitoxin is a family of approximately 24 compounds (3), and strains of *A. catenella* and other species produce different combinations of these congeners. Each isolate's profile, or fingerprint, is consistent across culture conditions (4), and thus is considered a constitutive marker for given strains or populations in a region. In this context, toxin profiles collected from the western coast of the Bering Sea (5) and in the Chukchi Sea (Fig. S1), combined with other profiles obtained from the Bering and Chukchi Seas isolates (6, 7) provide useful and interesting preliminary data for inferring the origin and connectivity of blooms in these regions. Figure S1 shows the saxitoxin profiles of isolates of *Alexandrium catenella* and the major currents in the Bering and Chukchi Seas. Several observations are of note. First, the Chukchi isolates in the Central Pathway (toxin profile #7 in Fig. 4; see 6) are strikingly different from those from the large cyst seedbed area in the Alaskan coastal current (ACC) region of the Chukchi (profiles #7 -9 in Fig. S1). No other isolates analyzed from the region have that distinctive Central Pathway fingerprint. In contrast, the Chukchi isolates from the ACC region most closely resemble populations from the western Bering Sea near the Kamchatka peninsula (e.g., profiles #3-4 in Fig. S1). One preliminary conclusion from this limited dataset would be that the large Chukchi cyst bed (Fig. 1) may derive from cells transported from Russian waters of the western Bering Sea via the Anadyr Current, and not those from the eastern Bering Sea (toxin profile #10, Fig. S1). Since saxitoxin is 3 to 15 times more potent than toxins GTX5 and C2 respectively, the relative inputs of bloom populations from these source waters would contribute to dramatic differences in overall toxicity and consequently determine the magnitude of ecosystem and human health impacts.

Detailed methods. Below are detailed methods and approaches used for data collection and analysis.

Plankton sampling and Alexandrium *hybridization.* At each station, 2 L of water were collected from Niskin bottle samples taken at the surface, 10 m and chlorophyll maximum Niskin bottles. Additional depths were sampled at locations where significant concentrations of *Alexandrium* cells were detected through shipboard microscopy or underway imagery. During HLY1901 and IERP, the underway seawater system was used to collect additional samples during transit. Water was sieved and concentrated on a 15 μm Nitex sieve, backwashed into a 15 mL conical tube, preserved with 0.75 mL formalin (5% final concentration), and stored at 1°C for up to 72 hours. Samples were centrifuged (3000 g x 10 minutes), seawater-formalin mixture was aspirated, and flocculent pellet was resuspended in ice-cold methanol and stored at -20°C.

Fluorescence *in situ* hybridization (FISH) was used to label and enumerate *Alexandrium* cells in the preserved field samples. The oligonucleotide probe NA-1 Cy3 (5' Cy3-AGT GCA ACA CTC CCA CCA-3')

was selected to target the North American ribotype *Alexandrium catenella* LSU rRNA. The FISH method ensures quick and accurate identification of *A. catenella* in samples that may be particle-dense or that contain morphologically similar dinoflagellates which can confound identification under traditional light microscopy. Following methods outlined in Anderson et al. (8), an aliquot of each methanol-preserved sample was concentrated onto a 25 mm Cyclopore membrane via vacuum filtration. Prehybridization buffer was applied (5X SET [750 mM NaCl, 5 mM EDTA, 100 mM Tris-HCL, ph 7.8], 0.1 μg ml^{-1} polyadenylic acid, 0.1% IGEPAL CA-630, 10% formamide) at a volume of 1.0 mL and allowed to incubate at room temperature for 5 minutes. Vacuum filtration was used to remove the solution, and 1.0 mL hybridization buffer was added (pre-hybridization buffer plus 4.8 μg mL^{-1} NA-1 probe). Samples were incubated in the dark for 1 hour at 50°C, hybridization buffer was removed via vacuum filtration and replaced with 1.0 mL wash buffer (0.2X SET) for five minutes at room temperature. Filters were mounted on microscope slides using 80% glycerol in 25X SET and stored at 4°C until enumeration. All samples were analyzed within 72 hours of hybridization. Each filter was examined on a Zeiss Axioscope M1 at a 10x objective coupled with a Cy-3 filter set (Chroma #49016/TRITC Long pass), all positively-labeled *Alexandrium* cells were enumerated.

Sediment collection and cyst enumeration. Sediments used for quantitative analysis of *Alexandrium* cyst abundance were collected via Van Veen grab at each station. A syringe was used to draw a 16-cc plug of sediment, representing the 0-3 cm layer, from the surface of the grab. For samples collected during the IERP cruise, several plugs from the 0-3 cm layer were homogenized prior to analysis. This sediment was homogenized and stored in an airtight container, which was maintained in the dark at 1-4°C for the duration of the cruise. Upon cruise conclusion, samples were transported to the laboratory on blue ice, care was taken to ensure that sediments neither froze nor warmed significantly during transport.

Samples were processed following protocols outlined in Anderson et al. (8). A subsample of each plug was diluted 1:5 in filtered seawater and this dilution was sonicated with a Branson Sonifier 250 at a constant 40% amplitude for one minute in order to disaggregate cyst and sediment clumps. Sediments were sieved to isolate the 20-80μm size fraction, which was resuspended to 15mL in seawater and fixed with formalin (5% final). After 1-3 hours of refrigeration at 4°C, samples were centrifuged (3000 g x 10 minutes), formalin solution was aspirated, and sediment pellets were resuspended in 10 mL methanol and refrigerated at 4°C for 72 hours. In order to stain cysts for observation (10), methanol-preserved sediments were centrifuged and methanol was aspirated, sediments were resuspended in 10 mL deionized water. Centrifugation and aspiration were repeated and samples were resuspended in 2 mL primuline stain (2 mg mL^{-1}). Sediments were incubated in the dark for one hour at 4°C on a Labquake rotator. Following incubation, each sample was brought to 10 mL with deionized water, centrifugation and aspiration was repeated, and a final deionized water resuspension and centrifugation step was conducted before resuspending sediments to a final volume of 10-15 mL in deionized water. One milliliter of sample was loaded in to a Sedgewick-Rafter chamber and *Alexandrium* cysts were enumerated using a Zeiss Axioscope epifluorescence microscope at 10x objective under a FITC filter set (Zeiss 09, excitation = [450-490] nm BP; emission = [515] nm LP). Samples that were too dense with cysts or sediment for accurate counting were diluted 1:10 prior to final enumeration, all cyst counts were normalized to cysts per cubic centimeter (cysts cc^{1}). Only intact cysts were included in final counts.

In order to estimate overall cyst abundance within the study region, cyst data from all cruises were combined, with repeat stations averaged, to create a composite cyst dataset. To determine cyst bed scale, the area corresponding to cyst concentrations greater than 300 cysts cc^{1} was estimated using a gridded lateral map of cyst abundance (see below for a description of the gridding procedure). This was used to estimate the total cyst load within the top 3 cm of each cyst bed region as well as across the entire study area.

Hydrographic analyses. Conductivity-temperature-depth (CTD) data were collected during HLY1801, HLY1901, and HLY1803, using *Healy*'s Sea-Bird 911plus CTD. For each cruise, the CTD was configured to measure temperature and conductivity (dual sensors), pressure, oxygen, beam transmission, fluorescence, and photosynthetically active radiation. The CTD was mounted on a 24-position rosette with 10-liter Niskin bottles. Bottle salinity samples were taken for conductivity sensor assessment and calibration when appropriate. Laboratory calibrations for CTD sensors were performed by the manufacturer prior to and after each field season. As per manufacturer recommendations, CTD data were

processed using SeaBird data processing software (ver. 7.22.0). The raw CTD data were converted from HEX to ASCII, lag corrected, edited for large spikes, smoothed according to sensor, and pressure averaged into 1 db bins for final data quality control and analysis.

Final data quality control included minor hand-editing of data to address any remaining physical inconstancies (e.g., biofouling of sensors and small density inversions). Sufficiently deep CTD casts were performed during HLY1801 and HLY1803 allowing salinity samples to be used for post-calibrating the CTD conductivity sensors. Salinity samples taken during HLY1901 were used to ensure sensor health and provide qualitative assurance of manufacturer calibrations. Due to a lack of deep CTD casts on that cruise, no post-calibration of the conductivity sensors was performed. Instead, primary and secondary temperature and conductivity measurements were regressed against one another in order to verify performance. Resulting data quality from all cruises was excellent, and downcast 1-db pressure-averaged files had resulting accuracies near 0.001°C for temperature and 0.002 for salinity.

Shipboard ADCP database. The shipboard ADCP (SADCP) dataset includes 33 cruises from USCGC *Healy*, and 7 cruises each from R/V *Sikuliaq* and R/V *Mirai* collected between 2002 and 2018. All *Sikuliaq* cruises, and *Healy* cruises after 2004, were collected with the Univ. of Hawaii UHDAS software. This generates a near-final product in real-time by applying standard processing steps with default settings tailored for each ship. These include bottom- and water-track calibrations, single- and ensemble-ping editing, as well as checks on the applied ship's heading against additional heading feeds. A subset of these cruises had previously received additional post-cruise processing as part of other research projects. The data from the remainder of the cruises were visually edited for standard issues such as remaining bottom or ice interference. Previously applied calibrations and heading corrections via secondary heading feeds were checked, and in a few cases slightly adjusted.

The *Mirai* and the 2002-04 *Healy* SADCP data had been collected with VMDAS. Processed data were kindly provided by M. Itoh and A Münchow, respectively. Both sets were further edited, based in large part on considering standard status variables. These included "percent good" (PGOOD, the fraction of pings accepted by the ADCP to include in ensemble averages, typically about 5 minutes long), backscatter amplitude, and "error velocity" (a combination of the four along-beam velocities that cancels out for a velocity field that is constant within the ensonified area). For the *Mirai*, a subjective quality flag had been added by the data processor that correlated most closely with PGOOD. The flag value 8 for "bad" was never set, but 4 for "questionable" proved a useful guide for including velocity estimates. Only on- station data were used for the 2017 cruise due to a calibration problem that could not be corrected without additional data. Small portions of other cruises were removed for excess noise triggered by configuration tests that included vertical bins as small as 4 m for an Ocean Surveyor 75 kHz instrument where the default is 16 m.

A significant portion of the 2002-04 *Healy* underway data was edited out as well. The dataset included a parameter to indicate the fraction of pings per ensemble (0 to 100) for which ADCP bottom-track (BT) or GPS-based navigation information had been used during the conversion from ship- to earth-relative velocity estimates. Under BT, possible transducer misalignments or heading errors cancel out as they affect both the velocity profiles and the reference velocity. Correspondingly, underway and on- station data looked similar under BT referencing. There were significant differences, however, for GPS-based navigation. This affected all deep portions where the bottom was out of the ADCP range, but also large parts of the shallower track where BT was not used.

A concern for all ships was the so-called "forward bias" – under poor conditions, the measured ADCP velocity relative to the transducer can drift towards zero. Combined with the ship velocity, this produces a bias in the direction of the ship's motion. Vessels with ice classifications can be more prone to such errors as their hulls tend not to have fairings or other obstacles that may shield transducers from bubble layers. Forward bias may be clearly visible when the ship track includes stops and turns, such as along a CTD transect. It can be very difficult to distinguish from actual current signals during long, fairly straight transits, which unfortunately includes large portions of our data. We adopted a conservative approach to transit data, basically requiring additional evidence that they were good rather than only looking for obvious errors. As a result, significant portions, but not all, of transit data from all cruises were edited out.

Historical hydrographic database. Water column hydrographic profile data were from the compilation described in Danielson et al. (11) and included primarily CTD, bottle, and profiling float soundings from

the National Centers for Environmental Information (NCEI) World Ocean Database 2018 (WOD18) (12). Additional profiles came from the US National Oceanographic and Atmospheric Administration (NOAA) Pacific Marine Environmental Laboratory (PMEL) and NOAA Alaska Fisheries Science Center (AFSC) hydrographic databases, the University of Alaska Fairbanks Institute of Marine Science (UAF IMS) hydrographic database, and CTD data compiled by the Synthesis for Arctic Ocean Research (13). Data from other nations were provided by Fisheries and Oceans Canada's Institute of Ocean Sciences (IOS) and the Japan Agency for Marine-Earth Science and Technology (JAMSTEC). All data were processed from raw form by the originating institutions. Our data screening procedures included the following additional thresholds. Data locations were screened for position and depth errors. Any station having salinity of less than 20 at 75 m depth or deeper was assumed to be unreliable and was discarded (this condition removed a number of faulty autonomous float profiles). We computed the freezing point and removed casts showing data that were supercooled by more than 0.1 °C (suggesting problems with conductivity sensor calibration). Temperature data were excluded outside a range of -2 to +25 °C and salinities outside a range of 0 to 38. We employ the Practical Salinity Scale, using the dimensionless practical salinity units (psu) for reporting all salinities.

Construction of lateral maps and vertical sections. To make the lateral maps, the data were interpolated onto a regular grid following the procedure used in Davis (14) and Våge et al. (15). For each grid pixel we considered the data points within an effective radius. Enhanced weighting was given to data in the along-isobath direction. This is appropriate given the predominantly barotropic circulation in the study region. For the temperature and velocity data, an effective radius of 30 km was used and the lateral grid spacing was 0.1°×0.1°. Since the biological (cyst and cell) data coverage is considerably sparser, an effective radius of 120 km was used, with a lateral grid resolution of 0.2°×0.2°. For the vertical sections, Laplacian-Spline interpolation (16) was used with a horizontal grid spacing of 10 km and a vertical grid spacing of 5 m.

Temperature gradient bar experiments. Laboratory experiments were performed to assess the effects of temperature on germination and growth responses of *A. catenella* under temperature conditions that bloom populations would experience during summer in the Alaskan Arctic.

Germination experiments were conducted with cyst-rich sediment collected from the Ledyard Bay area at LB-6 (69.584ºN, -165.7427ºE) and LB-8 (69.785ºN, -166.452ºE) on 22 August 2019 with a Van Veen grab. The sediment was stored at 0ºC until June 2020, when the experiment was carried out. Cyst-rich sediment was diluted with f/2 media to create a large, homogenized slurry for aliquoting. Slurry subsamples were delivered to 34 glass flasks as detailed in Anderson et al. (17). Four of these flasks were immediately harvested to determine the initial cyst concentration. The remaining flasks were randomly placed in incubators set to 0, 4, and 9ºC, as these temperatures reflect the climatology that cysts experience in situ in Ledyard Bay sediments. Illumination was set to 24-hrs at low light levels (~0.75 μmol $m^{-2}sec^{-1}$) to match light conditions experienced in the Ledyard Bay area during the summer months. Sampling intervals varied between incubation temperatures to ensure adequate coverage of the germination time course and ranged from 3 to 15 days. At each harvest interval, the flasks to be harvested were thoroughly rinsed and their contents were prepared for counting by staining with primulin as described by Yamaguchi et al. (18). All uncounted slurries were thoroughly mixed bi-weekly to provide consistent exposure to light and oxygenated media. To calculate the percentage of cysts that germinated over each time interval, the remaining cysts at each harvest interval were subtracted from the average initial cyst concentration.

Vegetative growth experiments were carried out with three isolates each from Greenland, Iceland, and the Chukchi Sea; three isolates originating from a temperate location, the Gulf of Maine (GOM), were also examined (See Richlen et al. (19) for details). These experiments were carried out using an aluminum temperature gradient bar, which was cooled at one end and heated at the other to provide a thermal gradient (2, 4, 6, 8, 12, 14, 16, 18, 20, 22, 24°C) with irradiance from below at 40 $\mu E/m^{-2}/s^{-1}$, and a 14:10 light/dark cycle. Cultures were slowly adjusted in a stepwise manner from standard conditions to experimental treatments (e.g., 2°C change every two days until the desired temperature was reached). Once culture was acclimated, 1 mL of ~5000 cells mL^{-1} culture was transferred into 25 mL of fresh, temperature equilibrated f/2 medium (thus, the inoculum cell density is 200 cells mL^{-1}) and placed in the temp-gradient bar. Population growth was monitored using in *vivo* fluorescence measured with a Turner Designs model 10-AU Fluorometer equipped with a 25 mm cuvette holder. Briefly, fluorescence was

measured in each tube at the same time every two days. The tubes were shaken to distribute the cell uniformly in the medium before measuring fluorescence. and tubes were shaken by hand to distribute the cells uniformly in the medium before measuring fluorescence. Growth data were collected from three technical replicates of each isolate.

The intrinsic growth rate was calculated over the exponential phase of growth (as inferred from a semi-log plot of fluorescence versus time (20,21) using the following equation:

$$\mu = \frac{\ln(N1/N0)}{t1 - t0}$$

in which μ (d^{-1}) represents the growth rate, and N1 and N0 represent the fluorescence at times t1 and t0, respectively.

SI References

1. L. K. Coachman, K. Aagaard, R. Tripp, Bering Strait: the regional physical oceanography, University of Washington Press (1975).
2. P. Lin, R. S. Pickart, L. T. McRaven, K. R. Arrigo, F. Bahr, K. E. Lowry, D. A. Stockwell, C. W. Mordy, Water mass evolution and circulation of the northeastern Chukchi Sea in summer: Implications for nutrient distributions, *J. Geophys. Res. Oceans* 127, 4416-4432 (2019).
3. A.D. Cembella, "Ecophysiology and metabolism of paralytic shellfish toxins in marine microalgae" in Physiological Ecology of Harmful Algal Blooms (D.M. Anderson, A.D. Cembella, G.M. Hallegraeff, Ed., (Springer-Verlag, 1988), pp. 381–403.
4. A.D. Cembella, J.J. Sullivan, G.L. Boyer, F.J.R. Taylor, R.J. Andersen, Variation in paralytic shellfish toxin composition within the *Protogonyaulax tamarensis/catenella* species complex; red tide dinoflagellates. *Biochem. Systematics and Ecol.,* 15, 171-186 (1987).
5. T. Y. Orlova, M. S. Selina, E. L. Lilly, D. M. Kulis, D. M. Anderson, Morphogenetic and toxin composition variability of Alexandrium tamarense (Dinophyceae) from the east coast of Russia, Phycol*.,* 46, 534–548 (2007).
6. M. Natsuike, H. Oikawa, K. Matsuno, A. Yamaguchi, I. Imai, The physiological adaptations and toxin profiles of the toxic Alexandrium fundyense on the eastern Bering Sea and Chukchi Sea shelves," Harmful Algae, 63, 13–22 (2017).
7. H. Gu, N. Zeng, Z. Xie, D. Wang, W. Wang, Morphology, phylogeny, and toxicity of Atama complex (Dinophyceae) from the Chukchi Sea. *Polar Biol* 36, 427-436 (2013).
8. D. M. Anderson, D. M. Kulis, B. A. Keafer, K. E. Gribble, R. Marin, C. A. Scholin, Identification and enumeration of *Alexandrium* spp. from the Gulf of Maine using molecular probes. *Deep Sea Res. II* 52, 2467-2490 (2005).
9. D. M. Anderson, B. A. Keafer, J. L. Kleindinst, D. J. McGillicuddy Jr., J. L. Martin, K. Norton, C. H. Pilskaln, J. L. Smith, C. R. Sherwood, B. Butman, *Alexandrium fundyense* cysts in the Gulf of Maine: long-term time series of abundance and distribution, and linkages to past and future blooms. *Deep Sea Res. II: Top. Stud. in Oceanogr.* 103, pp.6-26 (2014).
10. M. Yamaguchi, S. Itakura, I. Imai, Y. Ishida. A rapid and precise technique for enumeration of resting cysts of *Alexandrium* spp. (Dinophyceae) in natural sediments. *Phycol.* 34, 207-214 (1995).
11. S. L. Danielson, O. Ahkinga, C. Ashjian, E. Basyuk, L. W. Cooper, L. Eisner, E. Farley, K. B. Iken, J. M. Grebmeier, L. Juranek, G. Khen, Manifestation and consequences of warming and altered heat fluxes over the Bering and Chukchi Sea continental shelves. *Deep Sea Res. II: Top. Stud. in Oceanogr.*, 104781 (2020).

12. T. P. Boyer, O. K. Baranova, C. Coleman, H. E. Garcia, A. Grodsky, R. A. Locarnini, A. V. Mishonov, C. R. Paver, J. R. Reagan, D. Seidov, I. V. Smolyar, K. Weathers, M. M. Zweng, World Ocean Database. A. V. Mishonov, Tech. Ed. (National Centers for Environmental Information, 2018).
13. S. K. Moore, B. D. Bill, L. R. Hay, J. Emenegger, K. C. Eldred, C. L. Greengrove, J. E. Masura, and D. M. Anderson, Factors regulating excystment of *Alexandrium* in Puget Sound, WA, USA. *Harmful Algae* 43, 103–110 (2015).
14. R. E. Davis, Preliminary results from directly measuring middepth circulation in the tropical and South Pacific, *J. of Geophys. Res. Oceans* 103, 24619-24639 (1998).
15. K. Våge, R. S. Pickart, M. A. Spall, G. Moore, H. Valdimarsson, D. J. Torres, S. Y. Erofeeva, J. E. Ø. Nilsen, Revised circulation scheme north of the Denmark Strait, *Deep Sea Res. I*, 79, 20-39 (2013).
16. W. H. F. Smith, P. Wessel, Gridding with continuous curvature splines in tension. *Geophys.* 55, 293–305 (1990).
17. D. M. Anderson, C. A. Stock, B. A. Keafer, A. B. Nelson, B. Thompson, D. J. McGillicuddy Jr., M. Keller, P.A. Matrai, and J. Martin*, Alexandrium fundyense* cyst dynamics in the Gulf of Maine. *Deep Sea Research Part II: Topical Studies in Oceanography*, *52*, 2522-2542 (2005).
18. M. Yamaguchi, S. Itakura, I. Imai, Y. Ishida, A rapid and precise technique for enumeration of resting cysts of Alexandrium spp. (Dinophyceae) in natural sediments. *Phycol.*, 34, 207-214 (1995).
19. M. L. Richlen, O. Zielinski, L. Holinde, U. Tillmann, A. Cembella, Y. Lyu, D. M. Anderson, Distribution of *Alexandrium fundyense* (Dinophyceae) cysts in Greenland and Iceland, with an emphasis on viability and growth in the Arctic. *Mar. Ecol. Prog. Ser.* 547, 33-46 (2016).
20. R. R. Guillard, “Division Rates” in Handbook of Phycological methods: Culture methods and growth measurements, J. R. Stein, Ed. (Cambridge University Press, 1973), pp. 289-311.
21. M. Wood, R. C. Everroad, and L. M. Wingard, Measuring growth rates in microalgal cultures. *Algal culturing techniques* 18, 269-288 (2005).

Table S1. Research cruises and ships of opportunity.

Date	Cruise	Regions(s)	Sample types	Comment
Aug 2018	Distributed Biological Observatory-Northern Chukchi Integrated Survey (DBO-NCIS), HLY1801; USCGC *Healy*	N. Bering Sea, Chukchi Sea, Beaufort Sea	Plankton, Sediments	
Aug 2019	Distributed Biological Observatory-Northern Chukchi Integrated Survey (DBO-NCIS), HLY1901; USCGC *Healy*	N. Bering Sea, Chukchi Sea, Beaufort Sea	Plankton, Sediments	
Oct-Nov 2018	Arctic Observing Network Cruise, HLY1803; USCGC *Healy*	Chukchi Sea, Beaufort Sea	Sediments	Ship of opportunity
Aug-Oct 2019	Arctic Integrated Ecosystem Research Program Cruise (IERP)	N. Bering Sea, Chukchi Sea	Plankton, Sediments	Ship of opportunity
Aug-Sept 2019	Northern Bering Sea Cruise	N. Bering Sea	Sediments	Ship of opportunity
July 2010	Chukchi Sea	Chukchi Sea	Sediments	Collected by Dr. Haifeng Gu (see Gu et al. (17)

Figure Legends

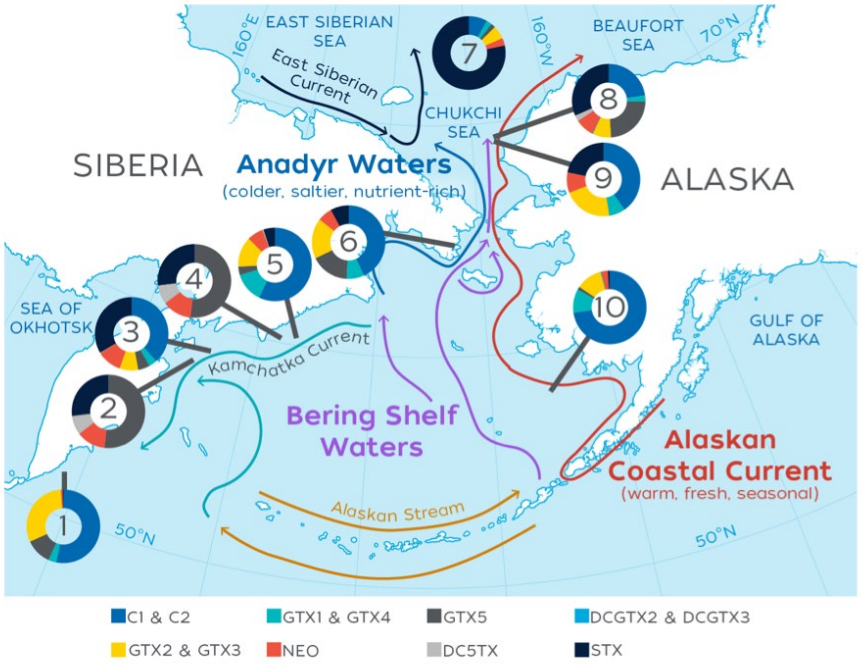

Figure S1. Map of the study area with *Alexandrium catenella* toxin composition profiles and major current pathways. Data sources cited in text.

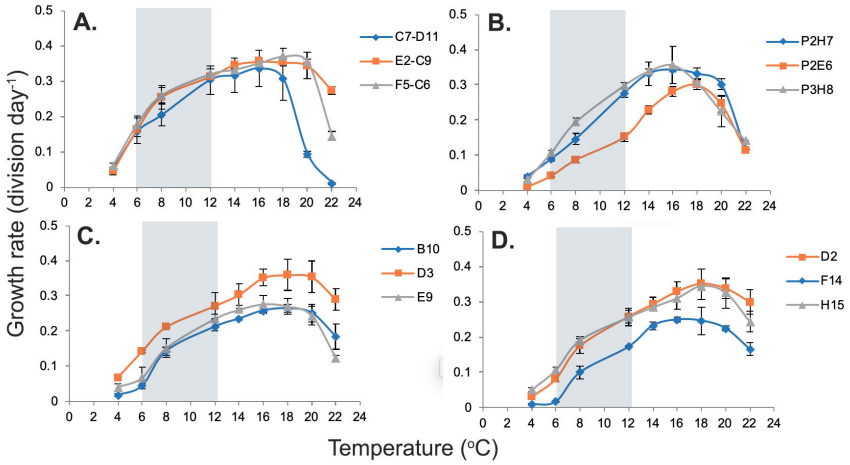

Figure S2. Growth rates of *Alexandrium catenella* strains isolated from the Chukchi Sea (A), Greenland (B), Iceland (C), and the Gulf of Maine (D) to temperature. The shaded gray bars represent the approximate range of surface water temperatures in the Chukchi Sea in 2018 and 2019 when *A. catenella* blooms were observed.

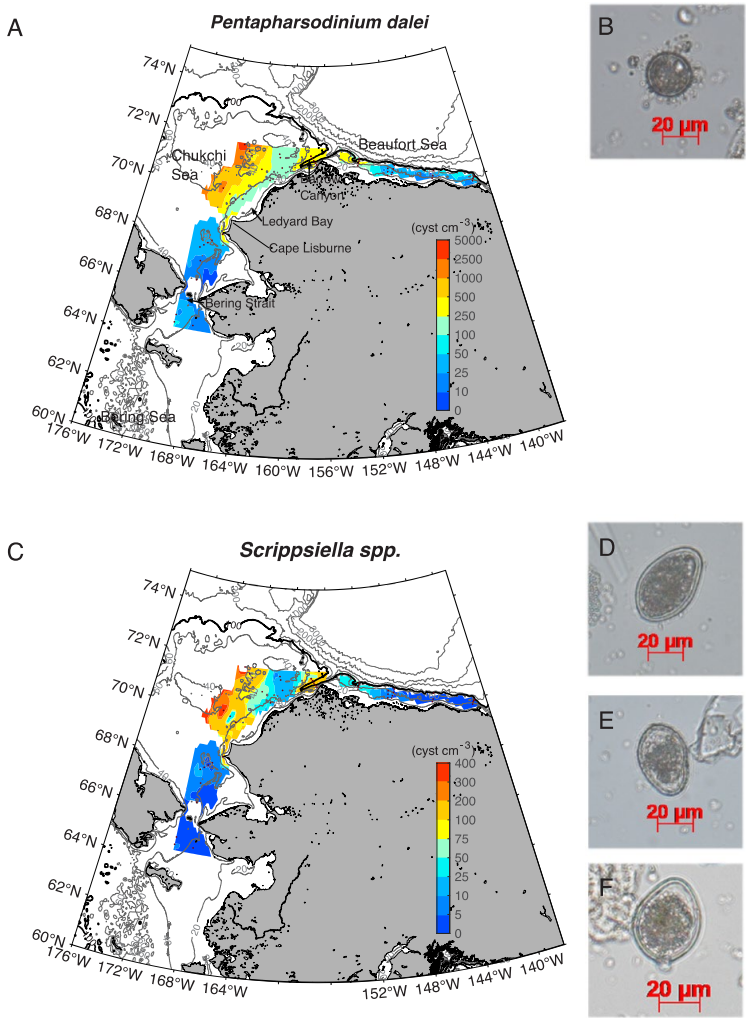

Figure S3. Spatial distribution of other dinoflagellate cyst species observed in sediments collected during 2018 surveys (HLY 1801, HLY 1803). Distribution of *Pentapharsodinium dalei* cysts (A) and example of *P. dalei* cyst captured under transmitted light (B). Distribution of *Scrippsiella* spp. cysts (C), a grouping which includes S. *lachrymose, S. crystallina*, and *S. trochoidea*. Examples of *Scrippsiella* spp. cysts captured under transmitted light (D-F)